Journal of Sound and Vibration 326 (2009) 623–632

Contents lists available at ScienceDirect

Journal of Sound and Vibration

journal homepage: www.elsevier.com/locate/jsvi

Friction-induced vibrations of squeal type due to transverse contraction in a flexible disk

B. Ryzhik *

LuK GmbH & Co. oHG, Industriestrasse 3, 77815 Buehl, Germany

ARTICLE INFO

Article history:
Received 10 November 2008
Received in revised form
4 June 2009
Accepted 9 June 2009
Handling Editor: C.L. Morfey

ABSTRACT

The mechanism of excitation of friction-induced vibrations in a system comprising a flexible annular disk and two rigid surfaces is studied analytically. The surfaces are pressed together, and the rotating disk slides between them. It is shown that the sliding friction in the contact between the disk and the surfaces, together with the transverse contraction in the disk material, set up a feedback between the orthogonal eigenmodes of the disk corresponding to the same eigenfrequency, thus initializing instability. The instability mechanism is illustrated by simple analytical considerations. The obtained results are confirmed by finite-element analysis.

1. Introduction

Squeal noise is a widespread phenomenon in engineering systems with a sliding contact. It is commonly acknowledged that the most probable instability mechanisms to initialize friction-induced vibrations of squeal type are mode-coupling or mode lock-in.

Numerous publications on the squeal phenomenon can be found in the literature. An overview of the publications on disk brake squeal is given, for example, by Kinkaid and O'Reilly [1]. A more general review on friction-induced vibrations is presented by Ibrahim [2]. Other authors [3–7] discuss a minimal model for studying the instability phenomenon. Several papers [8–13] (as well as many others) are devoted to modelling the contact pairs as multibody systems (MBS) or using finite-element methods. The effect of mode lock-in is discussed by a number of researchers, with several examples referred to [14–17]. Despite a wide range of investigations, some features of the investigated phenomenon that are important for the basic understanding of excitation mechanisms were not revealed, likely because of the complicity of considered systems.

In most applications, such as brake squeal or railway wheel squeal, the mode-coupling is a result of sliding contact between the elastic disk and elastic body. The elastic properties of both members of the contact pair influence the mode-coupling and complicate tracing the features of separate parts "responsible" for the instability.

In some engineering applications, the squeal appears due to the sliding contact between the elastic disk and rigid bodies. An investigation reveals that in such cases, the mode-coupling involves the eigenmodes of the disk itself. Due to axial symmetry, disks have an unlimited number of pairs of orthogonal eigenmodes; each pair corresponds to the same eigenfrequency. A sliding friction provides a feedback between these modes, which provokes instability.

One such instability mechanism is considered in the present paper. The prototype of the analysed system is a friction unit. The system includes a flexible disk made from plastic that moves by sliding between two steel surfaces, which can be considered as rigid. The disk dynamic deformation is restricted to in-plane vibrations. Due to transverse contraction

* Tel.: +49 7223 9414674; fax: +49 7223 9414799.
E-mail address: Boris.Ryzhik@schaeffler.com

0022-460X/$ - see front matter © 2009 Elsevier Ltd. All rights reserved.
doi:10.1016/j.jsv.2009.06.010

(Poisson's effect), the vibrations influence the normal force in contact and, consequently, the friction force. The change of the friction force in turn affects vibrations. This feedback leads to instability.

To illustrate the instability mechanism, a simple analytical model is considered. It is shown that due to the mode-coupling, the system is unstable in the first approximation; i.e., it has eigenvalues with positive real parts. Furthermore, the positive real parts are proportional under certain conditions to the friction coefficient and to Poisson's ratio. A more detailed finite-element analysis confirms the obtained results and enables to study the influence of system parameters on instability.

2. Instability mechanism

The analysed system is shown in Fig. 1. The system includes a homogeneous axial symmetric elastic disk and two rigid surfaces. The surfaces are pressed together, and the disk slides between them. There is a certain normal force in contact and, due to sliding, a corresponding friction force in the tangential direction.

The surfaces restrict the disk dynamic deformations to in-plane oscillations. The eigenmodes of the in-plane vibrations include a set of modes with k minima and maxima and $2k$ node lines ($k = 2, 3, \ldots$) in the circumferential direction. Due to axial symmetry, for each such mode there is an orthogonal mode with the same frequency (we assume that gyroscopic terms are small and have no influence on eigenfrequencies). The paired eigenmode has the same shape but different angular orientations, so the minima and maxima of the first mode are in position where the second mode has node lines (Fig. 2).

To a first approximation these modes represent a set of functions

$$\sin k\varphi,\ \cos k\varphi, \quad k = 2, 3, \ldots, \tag{1}$$

where φ is an angular coordinate in the polar coordinate system.

We suppose that without vibrations, the normal and tangential friction forces are uniformly (at least, axisymmetrically) distributed along the disk. Through radial vibrations, the disk has areas with elongation and compression. For example, by the dynamic deflection of the disk corresponding to the eigenmode presented in Fig. 2a, the areas of elongation and

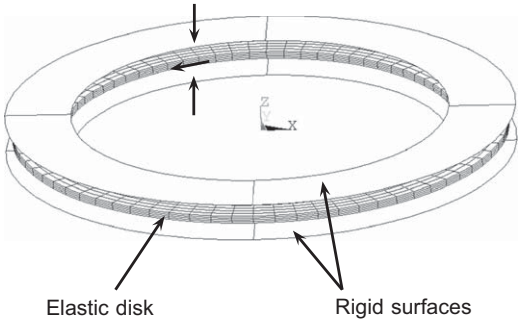

Fig. 1. Model of the system.

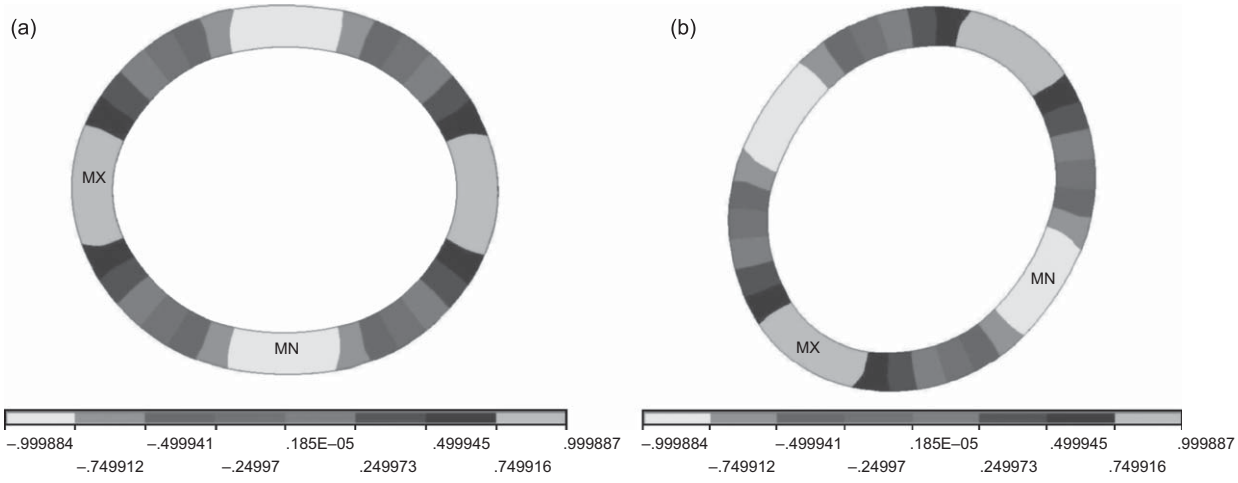

Fig. 2. Pair of eigenmodes with $k = 2$: (a) one of these modes, (b) paired mode.

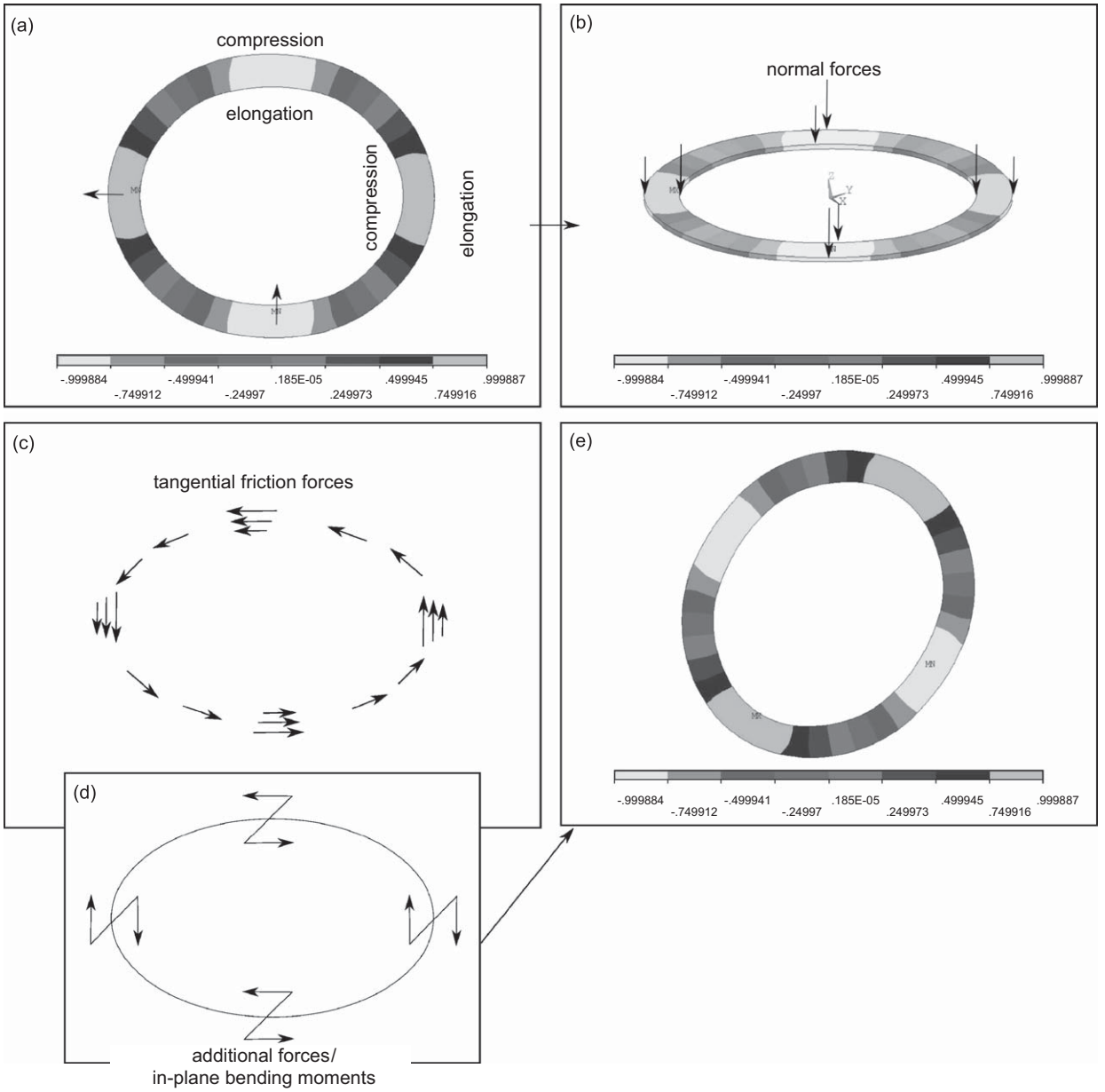

Fig. 3. Feedback between the paired eigenmodes: (a) areas of elongation and compression, (b) normal forces in contact, (c) tangential friction forces, (d) additional tangential forces and bending moments, (e) paired mode.

compression are situated according to Fig. 3a. Because of transverse contraction, this influences the normal force in contact. The disk will be "thinner" (decrease of the normal force) in the areas with elongation and "thicker" (increase of the force) in the areas with compression (Fig. 3b).

The alternation of the normal force changes the tangential friction force (Fig. 3c). The friction force decreases in the areas with elongation and increases in the areas with compression. Subtracting the uniformly distributed initial friction force, one can calculate an additional tangential force due to dynamic deflection. This force has reverse directions in the areas with elongation, and compression and builds an in-plane bending moment with a certain sign near maxima and an opposite sign near minima of deflection (Fig. 3d).

Such distribution of the additional tangential forces affects the dynamic deflection of the disk corresponding to the paired mode (Fig. 3e). The feedback between the eigenmodes with the same frequencies leads to instability.

Without damping, all modes of the type described by Eq. (1) would be unstable. The sources of instability are:

- axial symmetry of the disk, because of which the pairs of modes have the same eigenfrequency;
- friction with sliding and transverse contraction. Together they "set up" a feedback between the vibration modes.

3. Simple analytical model. Linear stability analysis

To investigate the instability mechanism, a simplified model of the system presented in Fig. 1 is analysed. The disk is considered as an annular beam with a small curvature. The equations of motion of such a system for the in-plane oscillations without damping and gyroscopic terms can be presented in the form (for example, as in Vibrations in Engineering [18])

$$\frac{\partial^6 y}{\partial\varphi^6}+2\frac{\partial^4 y}{\partial\varphi^4}+\frac{\partial^2 y}{\partial\varphi^2}+\rho\frac{R^4}{EI}\frac{\partial^2}{\partial t^2}\left(\frac{\partial^2 y}{\partial\varphi^2}-y\right)=-\frac{R^3}{EI}\left[\frac{\partial^2 m}{\partial\varphi^2}+m-R\left(\frac{\partial q}{\partial\varphi}-\tau\right)\right],$$

$$x=\frac{\partial y}{\partial\varphi}, \tag{2}$$

where $x=x(\varphi,t)$, $y=y(\varphi,t)$ are the dynamic displacements in radial and tangential directions, respectively, as functions of the angle φ in the polar coordinate system and time t, $q=q(\varphi,t)$, $\tau=\tau(\varphi,t)$ are the distributed radial and tangential forces, respectively, $m=m(\varphi,t)$ is the distributed in-plane bending moment, ρ, I are the linear density and the axial moment of inertia, respectively, of the beam cross-section, E is Young's modulus, R is the radius.

The tangential force includes the friction force τ_f and the external load τ_e, which enforce the disk rotation; the radial force is the part of the friction force caused by radial vibrations of the disk. It is assumed that the friction is of a Coulomb type and that, due to the rotation of the disk, sliding takes place.

The value of the friction force by sliding depends on the normal force in contact. The direction of the friction force coincides with the direction of the relative velocity. We suppose that vibration velocities are small compared to the speed of the rigid body motion of the disk. It is thus possible to neglect the small changes in the direction of the friction force and assign $q=0$.

Due to transverse contraction (Poisson's effect), the radial vibrations influence the normal force in contact. The dependence between the distributed normal force and the deformation of the disk is nonlinear. However, as a first approximation, this dependence can be linearized with the help of contact stiffness C_p. The corresponding friction force and the in-plane moment resulting from the dynamic deformation of the disk can then be calculated as

$$\tau_f=\int_{-b/2}^{b/2}(\theta_{f1}+\theta_{f2})\,\mathrm{d}u=-2\mu p_0 b,$$

$$m=\int_{-b/2}^{b/2}(\theta_{f1}+\theta_{f2})u\,\mathrm{d}u=-\mu\nu C_p\frac{I}{R^2}\left(\frac{\partial y}{\partial\varphi}+\frac{\partial^3 y}{\partial\varphi^3}\right),$$

$$\theta_{f1,2}=\theta_{f0}+\Delta\theta_{f1,2},\quad \theta_{f0}=-\mu p_0,\quad \Delta\theta_{f1,2}=-\mu\Delta p_{1,2},$$

$$p_{1,2}=p_0+\Delta p_{1,2},\quad \Delta p_{1,2}=C_p\Delta h_{1,2},$$

$$\Delta h_{1,2}=\tfrac{1}{2}\Delta h,\quad \Delta h=\Delta h(u)=-\nu\varepsilon h,$$

$$\varepsilon=\varepsilon(u)=-\chi u,$$

$$\chi=\frac{1}{R^2}\left(\frac{\partial y}{\partial\varphi}+\frac{\partial^2 x}{\partial\varphi^2}\right)=\frac{1}{R^2}\left(\frac{\partial y}{\partial\varphi}+\frac{\partial^3 y}{\partial\varphi^3}\right). \tag{3}$$

Here, $p_{1,2}$, $\theta_{f1,2}$; p_0, θ_{f0} represent the pressure and distributed friction forces, respectively, in contact with the upper and lower surfaces with and without additional deformation due to vibrations, Δh is the change of the beam thickness, $\Delta h_1=\Delta h_2$ is the one-sided "displacement" of the upper and lower surfaces due to deformation, χ, ε are the curvature and corresponding deformation, respectively, μ, ν are the friction coefficient and Poisson's ratio, respectively, u is the radial coordinate in the local coordinate system of the beam cross-section, and b, h are the length and the thickness of the cross-section, respectively (Fig. 4).

Using Eq. (3), we can rewrite the equation of motion as

$$\frac{\partial^6 y}{\partial\varphi^6}+2\frac{\partial^4 y}{\partial\varphi^4}+\frac{\partial^2 y}{\partial\varphi^2}+\rho\frac{R^4}{EI}\frac{\partial^2}{\partial t^2}\left(\frac{\partial^2 y}{\partial\varphi^2}-y\right)=-\frac{R^4}{EI}(\tau_e-2\mu p_0 b)+\frac{R}{E}\mu\nu C_p\left(\frac{\partial^5 y}{\partial\varphi^5}+2\frac{\partial^3 y}{\partial\varphi^3}+\frac{\partial y}{\partial\varphi}\right). \tag{4}$$

The motion of the disk can be divided into two parts: the rigid body motion $y_0=y_0(t)$ and the vibration part $\Delta y=\Delta y(\varphi,t)$

$$y=y_0+\Delta y,$$

$$\rho\frac{R^4}{EI}\frac{\partial^2 y_0}{\partial t^2}=\frac{R^4}{EI}(\tau_e-2\mu p_0),$$

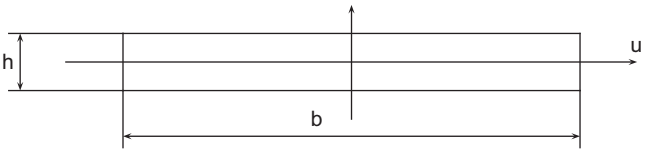

Fig. 4. Beam cross-section.

$$\frac{\partial^6 \Delta y}{\partial \varphi^6} + 2\frac{\partial^4 \Delta y}{\partial \varphi^4} + \frac{\partial^2 \Delta y}{\partial \varphi^2} + \rho \frac{R^4}{EI}\frac{\partial^2}{\partial t^2}\left(\frac{\partial^2 \Delta y}{\partial \varphi^2} - \Delta y\right) = \frac{R}{E}\mu v C_p \left(\frac{\partial^5 \Delta y}{\partial \varphi^5} + 2\frac{\partial^3 \Delta y}{\partial \varphi^3} + \frac{\partial \Delta y}{\partial \varphi}\right). \tag{5}$$

The equation for the vibration part is homogeneous. We search for a solution as a series

$$\Delta y(\varphi, t) = \sum_{k=2}^{\infty} [A_k(t) \sin k\varphi + B_k(t) \cos k\varphi]. \tag{6}$$

The index k in the summation starts from $k = 2$ because $k = 0, 1$ correspond to the rigid body motion of the disk.

Due to orthogonality of the functions $\sin k\varphi$, $\cos k\varphi$ the equations for $A_k(t)$, $B_k(t)$ for different indices can be separated

$$\ddot{A}_k + \omega_k^2 A_k - \mu v \alpha_k \omega_k^2 B_k = 0,$$

$$\ddot{B}_k + \omega_k^2 B_k + \mu v \alpha_k \omega_k^2 A_k = 0,$$

$$\omega_k^2 = \frac{EI}{\rho R^4}\frac{k^2(k^2-1)^2}{k^2+1},$$

$$\alpha_k = \frac{I}{\rho \omega_k^2 R^3} C_p \frac{k(k^2-1)^2}{k^2+1},$$

$$k = 2, 3, \ldots . \tag{7}$$

The characteristic equations of the system are

$$\begin{vmatrix} \lambda^2 + \omega_k^2 & -\mu v \alpha_k \omega_k^2 \\ \mu v \alpha_k \omega_k^2 & \lambda^2 + \omega_k^2 \end{vmatrix}, \quad k = 2, 3, \ldots . \tag{8}$$

Using the Routh–Hurwitz criterion, the stability condition for the trivial solution of Eq. (8) can be written as

$$\mu^2 v^2 \alpha_k^2 \omega_k^4 < 0, \quad k = 2, 3, \ldots . \tag{9}$$

The inequality equation (9) is never fulfilled; therefore, the system without damping is always unstable.

The eigenvalues of the system can be calculated directly by

$$\lambda = \pm \omega_k \tfrac{1}{2}\sqrt{2\sqrt{1+\mu^2 v^2 \alpha_k^2} - 2} \pm \mathrm{j}\omega_k \tfrac{1}{2}\sqrt{2\sqrt{1+\mu^2 v^2 \alpha_k^2} + 2}, \quad \mathrm{j} = \sqrt{-1},\ k = 2, 3, \ldots . \tag{10}$$

Each component with $k = 2, 3, \ldots$ has a pair of eigenvalues with a positive real part.

From Eq. (10), it follows that the modes of the type described by Eq. (1) are unstable. The value of real parts depends on the friction coefficient and on Poisson's ratio. If $\mu = 0$ or $v = 0$, the system would be stable.

When α_k is small, the corresponding eigenvalue can be approximately presented as

$$\lambda = \pm \tfrac{1}{2}\mu v \alpha_k \omega_k \pm \mathrm{j}\omega_k, \quad \mathrm{j} = \sqrt{-1},\ k = 2, 3, \ldots . \tag{11}$$

The value of positive real parts and the "level" of instability are in this case proportional to the friction coefficient and Poisson's ratio.

Damping can sufficiently influence the instability. The modes with a small positive real part may become stable (sign change of the real part); for the other modes, the real part will decrease. However, damping in the systems with sliding contact, especially with a steel-plastic contact, is a very uncertain variable. It depends on the frequency and amplitude of oscillations, contact forces, friction parameters and many other, often accidental, factors. Therefore, we choose to consider the system without damping to investigate the instability mechanism, keeping in mind that in reality, the system presumably will be distinctively more stable.

The instability conditions derived from Eq. (7) are rather simple, while, due to the axial symmetry of the disk, the terms $\omega_k^2 A_k$, $\omega_k^2 B_k$ in the first and second equations include the same frequency parameter ω_k^2. The terms "responsible" for the instability are $-\mu v \alpha_k \omega_k^2 B_k$, $\mu v \alpha_k \omega_k^2 A_k$. They characterize the coupling between the paired modes. These terms are

proportional to the friction coefficient and Poisson's ratio. This confirms the thesis of the previous section that the friction and transverse contraction induce a feedback between the paired modes, which leads to instability.

There is a certain difference between the squeal phenomenon in the brake system and that in the considered case. In the brake system, both members of the contact pair, the brake disk and the calliper with pads, are elastic, and the "interaction" between their dynamic properties influences the vibration mechanism.Typically, the system is stable for a low friction coefficient even without damping, and it becomes unstable only when the friction coefficient exceeds a certain "boundary value."

The considered system without damping is unstable for any non-zero friction coefficient and Poisson's ratio. The "level" of instability increases linearly with the growth of these parameters.

The analysed equations contain no gyroscopic terms. Usually, the rotational frequency by squeal of the considered type is very low compared to the frequency of squeal, and gyroscopic terms have no observable influence on instability.

4. Finite-element analysis

To prove the analytical conclusion about the instability of paired eigenmodes and to study the influence of system parameters, a finite-element analysis in ANSYS was carried out. The same system (Fig. 1) is considered. The disk is modelled as a 3-D elastic body; the surfaces are assumed to be rigid. The contacts on the lower and upper surfaces are defined using ANSYS options "surface-to-surface contact," "contact with rigid target" and "behaviour of contact surface standard." By the definition of contact, the friction coefficient is defined. The stability investigation is based on the results of Q-R-Damped modal analysis: calculation of the complex eigenvalues of the system taking into account the asymmetry of the elastic matrix due to friction.

In the previous section, we have studied the simplified system with unmovable rigid surfaces and a rotating disk; the disk was considered as free. The prototype of the analysed system is a friction unit with the motions of the disk being restricted. To take into account the realistic boundary conditions in finite-element analysis, we fix the disk in the tangential direction and move the surfaces to enable sliding. The swap of moving and unmoving parts does not affect the results of the presented stability analysis because the effects connected with rotation are not considered.

There are some possible variants of the disk fixation. We investigate the uniform fixation in the middle plane of the disk on the outer radius (Fig. 5). By other types of fixation, for example, by fixation only in some points on the outer radius, the numerical results could differ from those presented below, but the conclusions about the influence of the friction coefficient and Poisson's ratio on instability remain the same.

We present the numerical results for three eigenmodes of the type described by Eq. (1) with $k = 2, 3, 4$. Due to the boundary conditions, the eigenfrequency of the mode with $k = 3$ for a wide range of parameters is lower than the frequency of the mode with $k = 2$.

Computations include three steps:

1. Pre-load in normal direction (static analysis). The surfaces are pressed on each other to create initial pressure.
2. Sliding in the tangential (rotational) direction (static analysis). A certain displacement in the tangential direction is defined for both rigid surfaces. The 3-D disk is fixed in the tangential direction on its outer radius. The displacement should be sufficiently large to provide the status of both contacts as "sliding," but not so large as to avoid convergence problems. To enable the calculation of the asymmetrical elastic matrix, the ANSYS command "nropt,unsym" should be applied.

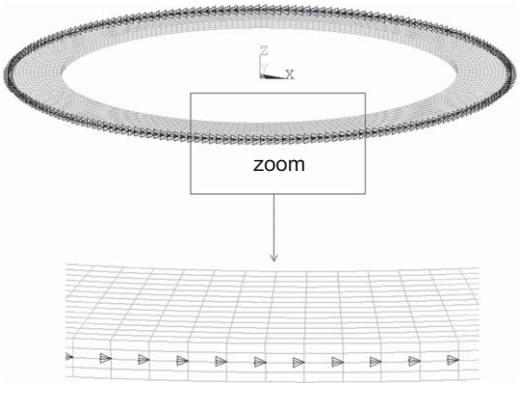

Fig. 5. Boundary conditions for the disk.

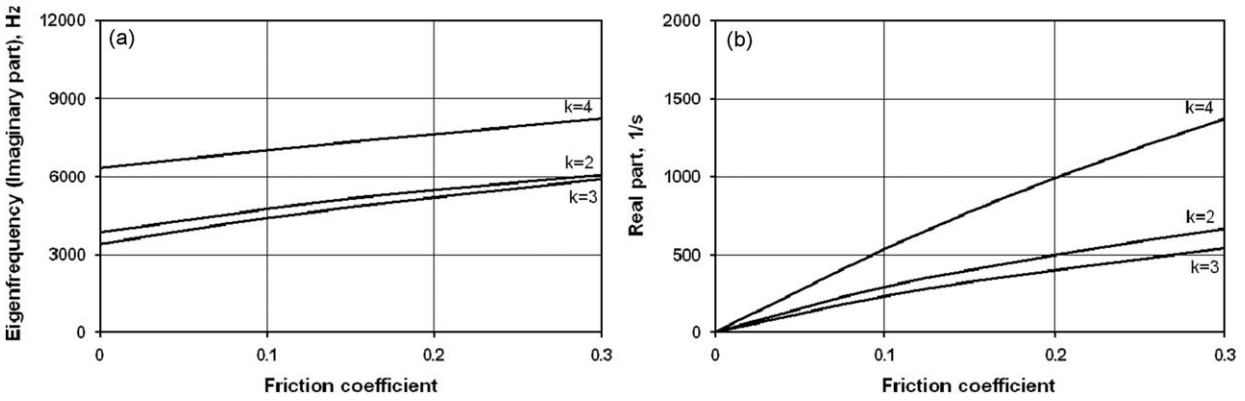

Fig. 6. Q-R Damped modal analysis: influence of the friction coefficient μ. Disk material: plastic, Poisson's ratio $\nu = 0.4$. (a) Eigenfrequencies vs. friction coefficient, (b) real parts vs. friction coefficient.

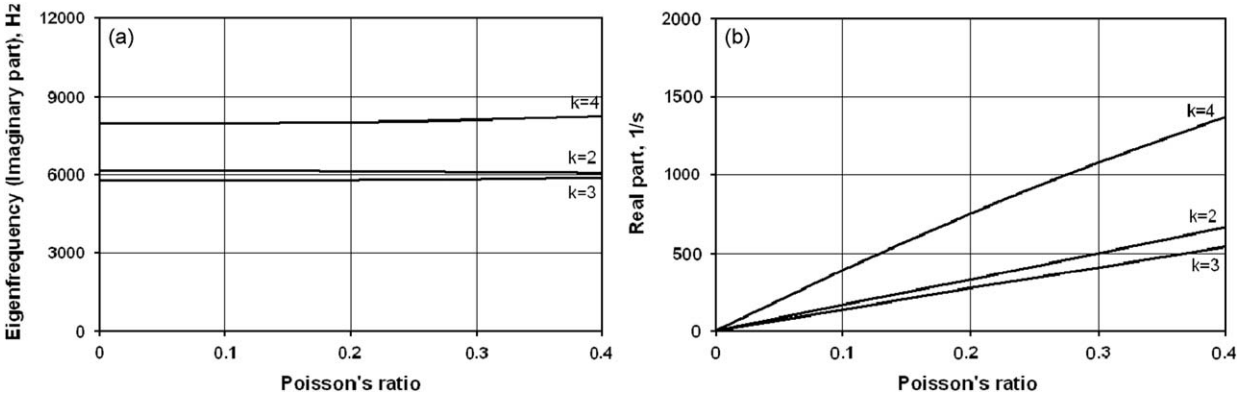

Fig. 7. Q-R Damped modal analysis: influence of Poisson's ratio ν. Friction coefficient $\mu = 0.3$. (a) Eigenfrequencies vs. Poisson's ratio, (b) real parts vs. Poisson's ratio.

3. Q-R-Damped modal analysis with the asymmetrical elastic matrix obtained by step 2. If some eigenvalues have a positive real part, corresponding eigenmodes are considered as "unstable."

The modal analysis is also performed without damping. Such an approach enables to estimate the "inclination" to instability for different eigenmodes by comparing the values of real parts.

The finite-element computations confirm in principle the analytical conclusions. All eigenmodes of the type described by Eq. (1) without damping are unstable: they have eigenvalues with a positive real part.

The influence of the friction coefficient is shown in Fig. 6. If $\mu = 0$, the system will be stable (has no eigenvalues with a positive real part). The rise of friction coefficient leads to the growth of both real and imaginary parts of eigenvalues. The system becomes noticeably more rigid (increase of eigenfrequencies) and more potentially unstable. The growth of positive real parts is almost linear, which corroborates the results of Section 3.

The variation of Poisson's ratio (Fig. 7) also confirms the prediction of the previous section: with an increase of ν, positive real parts of eigenvalues increase nearly linearly. If one found a hypothetical material with $\nu = 0$, the system would be stable. The influence of Poisson's ratio on the eigenfrequencies is minor.

The increase of the initial pressure leads to the growth of eigenfrequencies. The real parts of eigenvalues decrease slightly (Fig. 8).

The influence of geometrical parameters (thickness, width and radius of the disk) is investigated in Figs. 9, 10 and 11, respectively. One can see that the variation of thickness and width can sufficiently change both real and imaginary parts of eigenvalues. Furthermore, the "behaviour" of eigenvalues is different for the eigenmodes with different k. It is not possible to make general predictions about the optimal choice of geometrical parameters; in each concrete case, a numerical investigation should be carried out.

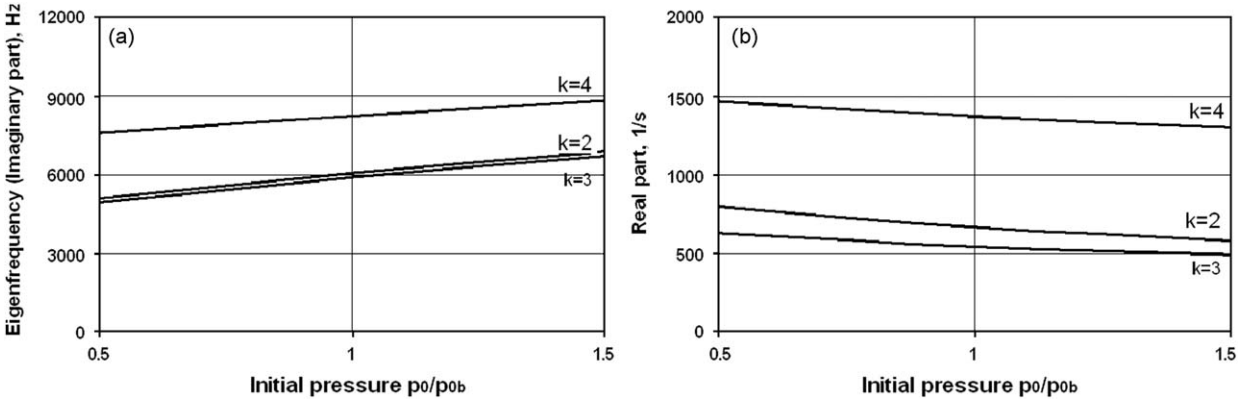

Fig. 8. Q-R Damped modal analysis: influence of the initial pressure p_0. Here, p_{0b} is the "basis" value of the initial pressure used in calculations in Figs. 6 and 7; $\mu = 0.3$, $\nu = 0.4$. (a) Eigenfrequencies vs. dimensionless initial pressure, (b) real parts vs. dimensionless initial pressure.

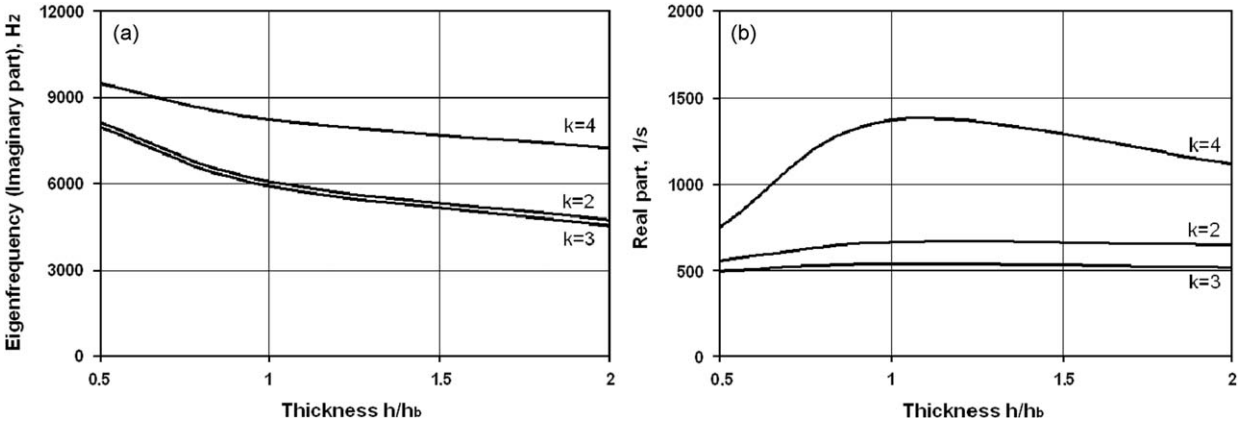

Fig. 9. Q-R Damped modal analysis: influence of the disk thickness h. Here, h_b is the "basis" thickness used in calculations in Figs. 6 and 7; $\mu = 0.3$, $\nu = 0.4$. (a) Eigenfrequencies vs. dimensionless thickness of the disk, (b) real parts vs. dimensionless thickness of the disk.

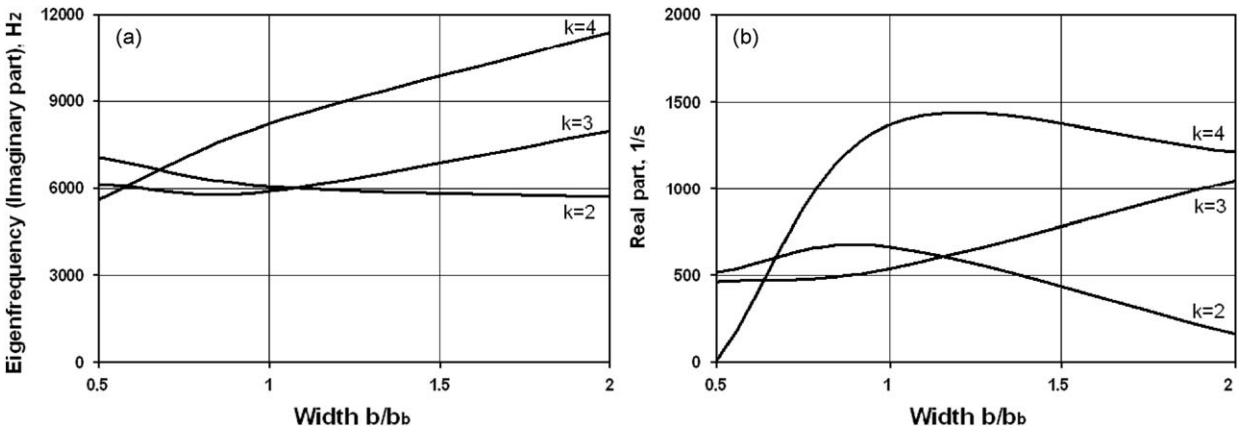

Fig. 10. Q-R Damped modal analysis: influence of the disk width b. Here, b_b is the "basis" width used in calculations in Figs. 6 and 7; $\mu = 0.3$, $\nu = 0.4$. (a) Eigenfrequencies vs. dimensionless width of the disk, (b) real parts vs. dimensionless width of the disk.

The most important result of the finite-element analysis is the conclusion that all eigenmodes of the type described by Eq. (1) without damping are unstable and that the values of positive real parts depend almost linearly on the friction coefficient and Poisson's ratio.

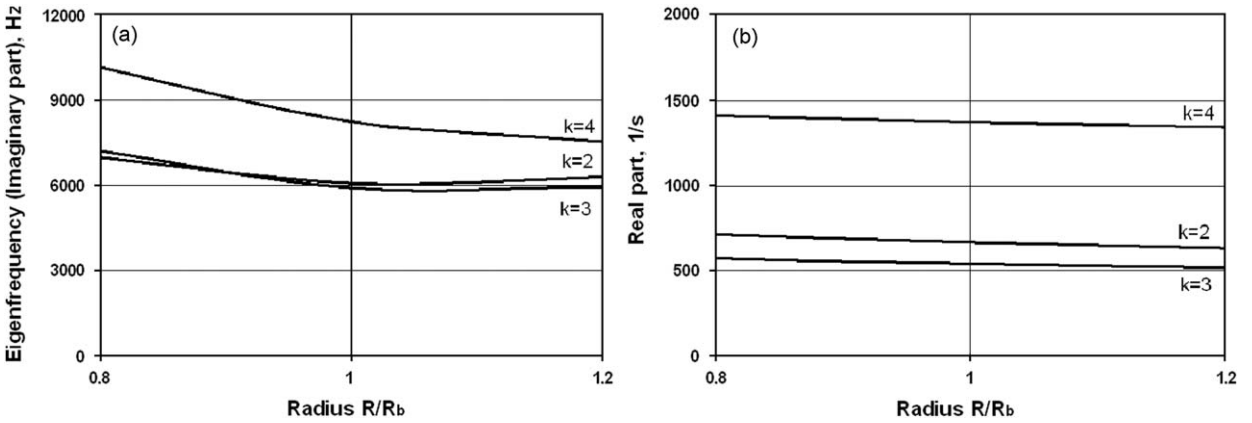

Fig. 11. Q-R Damped modal analysis: influence of the disk radius R. Here, R_b is the "basis" radius used in calculations in Figs. 6 and 7; $\mu = 0.3$, $\nu = 0.4$. (a) Eigenfrequencies vs. dimensionless radius of the disk, (b) real parts vs. dimensionless radius of the disk.

To estimate the influence of the rotational speed, some computations were carried out by applying the rotational velocity effect (ANSYS parameter Omega) and gyroscopic terms (Ansys parameter Coriolis) to the disk. The comparison of finite-element analysis results with and without these terms did not reveal any distinguishable difference.

In the case when all analysed eigenmodes have positive real parts, the introduction of damping causes a calculable effect because the models of damping available by FE Q-R-Damped modal analysis are rather simple. For example, if we introduced a Rayleigh damping proportional to the matrix of mass (the so-called alpha-damping, ANSYS parameter *ALPHAD*), all real parts of the eigenvalues would decrease by the same value. A similar situation occurs with the second option, Rayleigh damping proportional to the matrix of stiffness (beta-damping, BETAD).

5. Conclusion

A system consisting of a homogeneous elastic annular disk sliding between two rigid surfaces is studied analytically. It is shown that the transverse Poisson's contraction associated with the in-plane dynamic deformations of the disk sets up a feedback between the orthogonal eigenmodes of the disk corresponding to the same eigenfrequency, which can therefore provoke instability. The factors responsible for the instability are the axial symmetry of the disk, the sliding friction and the transverse (Poisson's) contraction.

The system without damping is unstable for any non-zero friction coefficient and Poisson's ratio. The tendency towards instability increases linearly with the growth of these parameters.

References

[1] N.M. Kinkaid, O.M. O'Reilly, P. Papadopoulos, Automotive disc brake squeal, *Journal of Sound and Vibrations* 267 (2003) 105–166.
[2] R.A. Ibrahim, Friction-induced vibration, chatter, squeal, and chaos, Part II: dynamic and modeling, *Applied Mechanics Reviews* 47 (1994) 227–253.
[3] K. Shin, M.J. Brennan, J.-E. Oh, C.J. Harris, Analysis of disk brake noise using a two-degree-of-freedom model, *Journal of Sound and Vibration* 254 (2002) 837–848.
[4] N. Hoffmann, M. Fischer, R. Allgaier, L. Gaul, A minimal model for studying properties of the mode-coupling type instability in friction induced oscillations, *Mechanics Research Communications* 29 (2002) 197–205.
[5] K. Popp, M. Rudolph, M. Kroeger, M. Lindner, Mechanisms to generate and to avoid friction induced vibrations, *VDI-Bericht* 1736 (2002).
[6] E. Brommundt, Ein Reibschwinger mit Selbsterregung ohne fallende Reibkennlinie, *Zeitschrift fur Angewandte Mathematik und Mechanik* 75 (11) (1995) 811–820.
[7] U. von Wagner, D. Hochlenert, P. Hagedorn, Minimal models for disk brake squeal, *Journal of Sound and Vibration* 302 (2007) 527–539.
[8] G. Chakrabotry, T. Jearsiripongkul, U. von Wagner, P. Hagedorn, A new model for a floating caliper disc-brake and active squeal control, *VDI-Bericht* 1736 (2002) 93–102.
[9] U. von Wagner, T. Jearsiripongkul, T. Vomstein, G. Chakrabotry, P. Hagedorn, Brake squeal: modelling and experiments, *VDI-Bericht* 1749 (2003) 173–186.
[10] J. Wauer, J. Heilig, Dynamics and stability of a nonlinear brake model, *Proceedings of ASME DETC*, 2001.
[11] J.E. Mottershead, H. Ouyang, M.P. Cartmell, M.I. Friswell, Parametric resonances in an annular disc, with a rotating system of distributed mass and elasticity; and the effects of friction and damping, *Proc. R. Soc. London* 453 (1997) 1–19.
[12] Q. Cao, H. Ouyang, M.I. Friswell, J.E. Mottershead, Linear eigenvalue analysis of the disc-brake squeal problem, *International Journal for Numerical Methods in Engineering* 61 (9) (2004) 1546–1563.
[13] G. Lou, T.W. Wu, Z. Bai, Disk brake squeal prediction using the ABLE algorithm, *Journal of Sound and Vibration* 272 (2004) 731–748.
[14] A. Tuchinda, N. Hoffmann, D. Ewins, W. Keller, Mode lock-in characteristics and instability study of the pin-on-disc system, *Proceedings of the International Society for Optical Engineering*, Vol. 4359 (1), 2001, pp. 71–77.
[15] M. Francisco, A. Akay, J. Wickert, The role of mode lock-in in generating brake noise and squeal, *Society of Automotive Engineers Brake Colloquium*, Philadelphia, PA, 1995.

[16] R. Allgaier, W. Keiper, L. Gaul, K. Willner, Mode lock-in and friction modeling, *Computational Methods in Contact Mechanics IV*, Southampton, WIT Press, 1999, pp. 35–48.
[17] R. Allgaier, L. Gaul, W. Keiper, K. Willner, N. Hoffmann, A study on brake squeal using a beam-on-disk model, *Proceedings of IMAC-XX*, 2002, pp. 528–534.
[18] F. Dimentberg, K. Kolesnikov, *Vibrations in Engineering*, Vol. 3, Moscow, Mashinostroenie, 1980 (Handbook in 6 volumes, in Russian language, re-issued 1995).